J Mater Sci (2009) 44:4944–4952
DOI 10.1007/s10853-009-3755-6

Descriptive microstructure and fracture surface observations of fired volcanic ash

C. Leonelli · E. Kamseu · U. C. Melo · A. Corradi · G. C. Pellacani

Received: 20 March 2009 / Accepted: 15 July 2009 / Published online: 4 August 2009

Abstract Crystals of the pyroxene group (diopside, augite and enstatite, hedenbergite), series of crystals with the general formula $(Mg_xFe_{1-x})_2SiO_4$ having various geometry, identified as spinel (and olivine), and plagioclase crystals from anorthite to anorthoclase that grow together in mass having thin parallel groves embedded in a complex matrix together with calcium alumina silicate grains were found to be the descriptive microstructure of fired volcanic ash. Quartz grains were rarely present as confirmed by dilatometry analysis, XRD, SEM and DTA. The presence of dendrites continuously growing to pyroxene crystals indicated the precipitation/crystallization of these crystals from matrix and regions of glass concentration enhance by ions diffusion. Rings of Ti-rich iron micro-crystals observed around spinel (and olivine) suggested the probable nucleating role of these micro-crystals for the precipitation/crystallization phenomenon. The various types of crystals formed, the difference in their geometry and size and their interlocking mechanism result in a contiguous and dense structure with relevant characteristics at relative low temperature (1125–1150 °C) confirming volcanic ash as a promising alternative raw material for vitrified ceramic products. It was concluded that controlled precipitation/crystallization of raw volcanic ash results on microstructure similar to that of glass-ceramic materials. The observation of fracture surface allowed comparison of fracture mechanics of volcanic ash ceramic to that of conventional vitrified ceramics.

C. Leonelli · E. Kamseu (✉) · A. Corradi · G. C. Pellacani
Department of Materials and Environmental Engineering, University of Modena and Reggio Emilia, Via Vignolese 905-41100, Modena, Italy
e-mail: kamseuelie2001@yahoo.fr; elie.kamseu@unimore.it

E. Kamseu · U. C. Melo
Laboratory of Materials, Local Materials Promotion Authority, 2396 Yaoundé, Cameroon

Introduction

The chemical system $CaO–MgO–Fe_2O_3–Al_2O_3–SiO_2$ has been the subject of extensive investigation [1–10]**.** In recent works [9, 10], we concentrated our attention on the sintering behavior and ceramic properties of fired volcanic ash noting their interesting mechanical properties and good densification behavior. It has been possible to obtain highly dense and resistant materials at relatively low temperature (1125–1150 °C). These attractive properties gave rise to investigation on the detailed microstructure. We wish to describe the potential crystalline phases formed as a function of the thermal treatment to complete the part of investigation on the suitable thermal cycle for better microstructure and mechanical properties of fired volcanic ash. Hence, fracture surface of fired volcanic ash is analyzed by SEM observations. These observations are correlated to the analysis of Young's modulus and the microstructure of the materials under indentation tests.

Methods

Experimental procedure

The samples of volcanic ash investigated in this study were selected among six used in the previous works [9, 10]. The two samples Z4 and Z6 were identified to be representative of the two groups resulting from the classification of the first study [9]. The natural wastes were all collected in the western region of Cameroon. The descriptive study of

Table 1 Thermal and mechanical properties of fired samples of volcanic ash

Samples	Thermal cycle	Thermal expansion (%)	Coefficient of thermal expansion $\times 10^{-6}$ K^{-1}			Micro hardness (Hv)		Young's modulus, E (GPa)	Fracture toughness (MPa $m^{1/2}$)
			20–100 °C	20–200 °C	20–1000 °C	1 N	5 N		
P1	Z4, 1125 °C, 5 °C/min, 0 h	1.10	6.50	7.77	9.79	831.63 ± 50.00	595.34 ± 33.26	109.11 ± 10.45	1.57 ± 0.10
P2	Z4, 1125 °C, 5 °C/min, 1 h	1.14	6.70	7.89	9.84	778.44 ± 51.12	509.11 ± 36.98	101.14 ± 9.64	1.52 ± 0.10
P3	Z4, 1150 °C, 10 °C/min, 2 h	1.22	7.73	9.43	10.53	730.08 ± 48.3	489.35 ± 40.78	92.87 ± 11.32	1.47 ± 0.10
P4	Z6, 1150 °C, 5 °C/min, 0 h	1.13	6.91	9.12	10.17	800.13 ± 47.99	586.41 ± 43.62	100.91 ± 12.44	1.53 ± 0.10
P5	Z6, 1125 °C, 5 °C/min, 2 h	1.08	6.30	7.30	9.97	845.13 ± 50.12	594.53 ± 51.23	115.46 ± 8.24	1.59 ± 0.10
P6	Z6, 1125 °C, 5 °C/min, 4 h	0.93	6.13	7.08	8.93	889.28 ± 49.94	622.34 ± 40.99	118.11 ± 8.54	1.56 ± 0.10

the microstructure of fired volcanic ash was in the direction of the investigation of sintering behavior initiated with the principal objective to evaluate the influence of thermal cycle on the ceramic products from volcanic ash.

Finely ground powder of volcanic ash (Z4 and Z6) were pressed (29 bars) to obtained discs with 40 mm diameter and 5 mm thickness. The specimens pressed were fired following the thermal cycles described in the Table 1 after having been left in oven (105 °C) for about 12 h.

Analytical

Contact less dilatometry measurements were performed on shaped fired volcanic ash specimens (5 × 5 × 15 mm) at a heating rate of 10 °C/min up to 1150 °C using an optical microscope (ESS MISURA HSM ODHT model 1600/80) that acquires the sample profile as function of temperature. The linear thermal expansion coefficient is also electronically elaborated taking the length (height) modification in the sample with temperature. The error in such measurement is about 0.6 μm, which is the minimum variation observable by the telecamera. The dilatation coefficient was directly calculated by the software coupled to the dilatometer. The XRD of fired specimens was evaluated using a diffractometer with goniometer PW3050/60 (theta/theta), Ni filtered Cu Kα radiation (40 kV, 40 mA). The microstructure of the fired specimens was studied by scanning electron microscopy (PSEM500, PHILIPS XL30) on fresh fractures (polished and no), etched and gold coated sections. The microanalysis of crystalline and the related phases were performed using EDS coupled to SEM.

Vickers microhardness, Hv (GPa), measurements were performed using the indentation technique at different loads (1–10 N) with an approach speed of 6 mm min^{-1}. The samples used for indentation analysis were prepared with the same method with those used for SEM analysis without etching. The depth range was 100 μm. For each experiment, 20 indentations were performed and the results statically analyzed in the aim to understand the influence of micro heterogeneity on the mechanical properties of fired volcanic ash. Analysis was performed using CSM instruments: indenter coupled to a micro-camera and software for image elaboration and analysis of indentations.

The elasticity Young's modulus, E (GPa), was calculated automatically for each indentation by the software from the Hv/E ratio, applying the equation given by Marshal et al. [11]. The fracture toughness Kc (MPa $m^{1/2}$) was determine by the equation:

$$Kc = \xi\left(\frac{E}{Hv}\right)^{1/2}\frac{P}{C^{3/2}},$$

where ξ is a material-independent constant, 0.016 for Vicker-produced radial crack, E/Hv is the modulus to hardness ratio, P is the indentation load (N) and c the indentation crack length (m).

Results

Crystalline phases

Diffraction lines attributed mainly to enstatite (Mg, Fe)SiO_3, augite (Ca(Mg, Fe)Si_2O_6, diopside (Ca(Mg, Al)(Si, Al)$_2O_6$, hedenbergite (Ca(Fe, Mg)Si_2O_6) as minerals of the pyroxene groups, spinel (ferromagnesian silicates), olivine (Fe_2SiO_4, (Fe, Mg)$_2SiO_4$)) and plagioclase (anorthite (Ca, Na)$AlSi_3O_8$), anorthoclase ((Ca, K)$AlSi_3O_8$) were identified (Fig. 1). In addition, calcium alumina silicates, pyroxferrite ($Fe_{.86}Ca_{.14}$)SiO_3 and other minor ferro crystals were observed. The similarity between peaks makes it

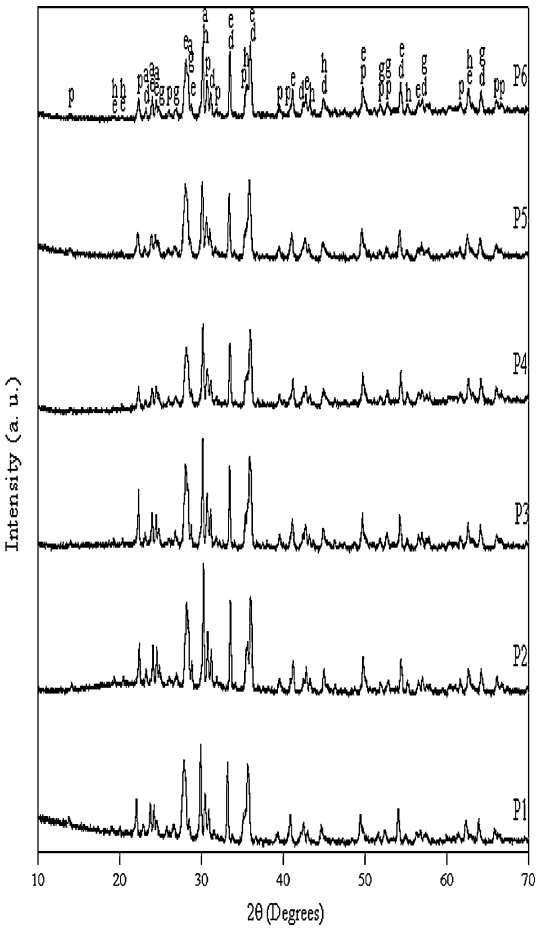

Fig. 1 XRD patterns of Z4 and Z6 samples as function of thermal cycle. *d* diopside, *e* entastite, *h* hebendergite, *g* augite, *p* plagioclase

difficult to define with accuracy the identification of some minerals of the same groups as pyroxene: the enstatite-ferrosilite series ([Mg, Fe]SiO_3) contain up to 5 mol% of calcium and exists in three polymorphs, orthoenstatite, protoenstatite and clinoenstatite. Increasing the calcium content prevents the formation of the orthorhombic phases. There is a miscibility gap between pigeonite and augite compositions as well as arbitrary separation between augite and the diopside-hedenbergite ($CaMgSi_2O_6$–$CaFeSiO_2O_6$) solid solution.

The different thermal cycle applied were with the aim to complete the investigations [9, 10] on the suitable thermal cycles for the achievement of the better microstructure-mechanical properties correlation initiated in the previous work. From Fig. 1 it can be observed that no additional phase was ascribed to the thermal cycle variation. The crystalline phases remain those identified above. The thermal cycle influenced the peaks intensity which may be due to the variation of the amount of amorphous phase content and the relative difference in $Na_2O + K_2O$ content of the two materials. In general, Z6 showed more intense peaks compared to Z4. It ought to be related to the degree of crystallization. The dilatometry curves confirmed fired volcanic ash as low-quartz content materials following the absence of quartz transition. The thermal expansion was found to be a function of thermal cycle applied, varying from 0.93% for the specimen fired at 1125 °C at 5 °C/min with 4 h soaking time to 1.22% for the specimen fired at 1150 °C at 10 °C/min with 1 h soaking time. At the same temperature of 1150 °C, the different firing rate make variation from 1.10% expansion at 5 °C/min to 1.22% at 10 °C/min. Focus to the soaking time, at 1125 °C (5 °C/min), the thermal expansion was 0.93% at 4 h instead of 1.08% at 2 h. As it can be observed in Table 1, fast firing rate should induce more liquid phase that is responsible for the high thermal expansion. From the XRD and dilatometry analyses, it can be concluded that controlled sintering of volcanic can result in increase of intensity of crystalline phases by then in low thermal expansion behavior.

Morphology, structure and composition of micro-phases

Figure 2 reveals the crystalline behavior of the fired volcanic ash. The largest grains (50 μm) are those of $(Mg_xFe_{1-x})_2SiO_4$ composition system identified as spinel (ferromagnesian silicates) that crystallize in the cubic (isometric) system; the oxide anions arranged in a cubic close-packed lattice and the cations occupying some or all the octahedral sites in the lattice. The spinel has an imperfect octahedral cleavages and a conchoidal fracture. Spinel (and olivine) were also present in the small size consistent with our suggestion on the mechanism of precipitation and growth of these grains in the matrix with temperature development. Small grains (5–20 μm), described above as mainly enstatite (Mg, Fe)SiO_3 and augite ($Ca(Mg,Fe)Si_2O_6$, presenting tetragonal or hexagonal morphology are present. Figure 2b shows the spectrum of the different crystals identified in the matrix of fired volcanic ash. The structure and the complexity of the geometry of spinel (or olivine) could not facilitate their identification but their chemical composition as collected from the microanalysis of about 30 grains were described as in wt%: SiO_2, 42.43; MgO, 40.36; FeO + Fe_2O_3, 16.78 and CaO < 1 being closed to spinels studied by Aoki and Shibi [12]. The other crystals included various forms of pyroxene, diopside, enstatite and hedenbergite essentially as confirmed by the XRD, together with anorthite, calcium silicate and calcium alumino silicate grains dispersed in the matrix. Figure 2b shows typical spectrum of these crystals. At higher magnification (Fig. 3) pyroxene grains are more visible. They are interlocked with other crystalline phases resulting in a contiguous structure. Mass of crystals that have grown together with surfaces having thin parallel groves is observed. Mass with chemical composition similar to that of

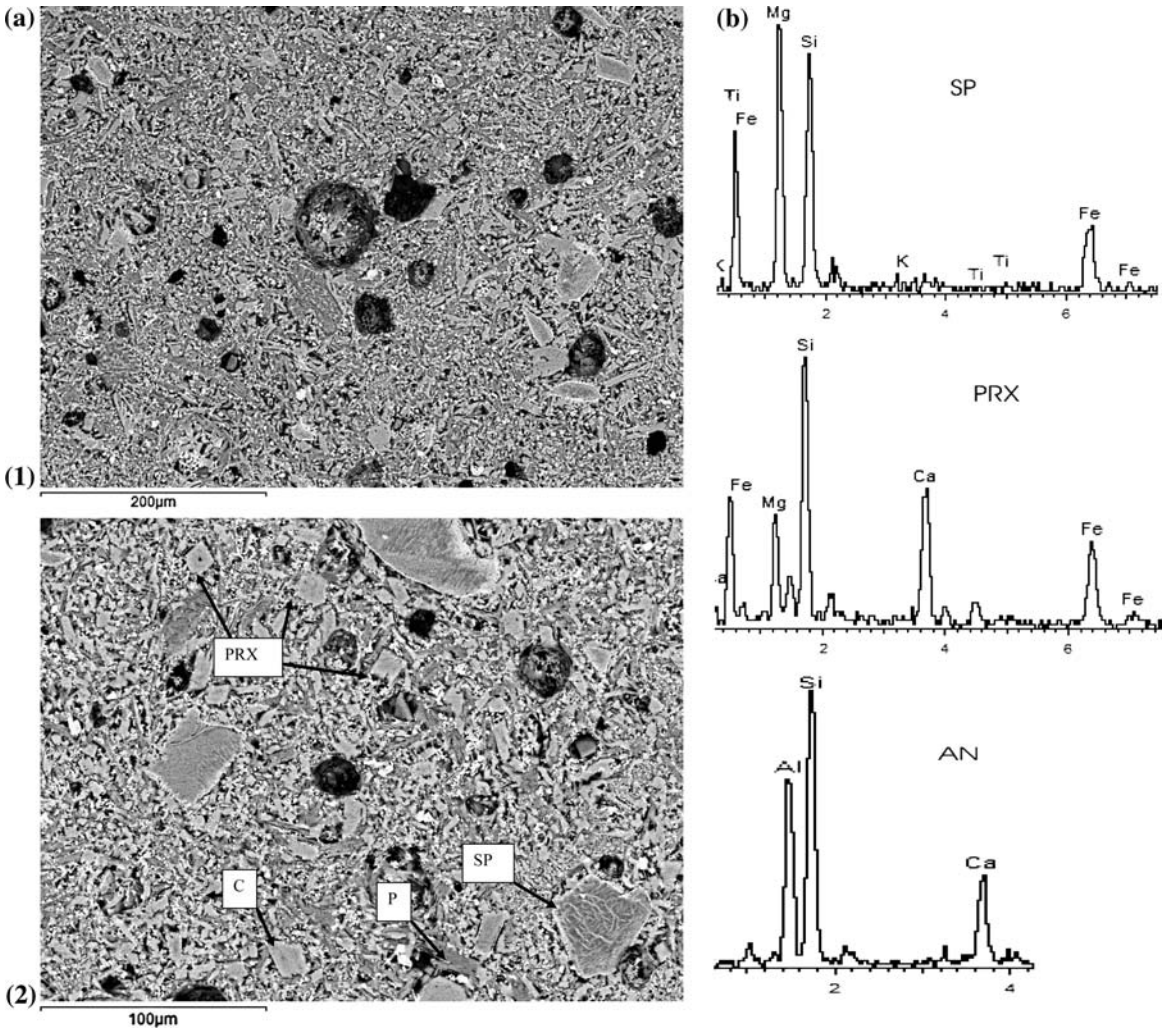

Fig. 2 **a** Crystalline phases in the matrix of volcanic ash **1** (P1), **2** (P4): *SP* spinel, *C* calcium alumina silicate, *P* plagioclase (anorthite), *PRX* pyroxene. The matrix is essentially continuous mass of plagioclase crystals that growth together in which pyroxene and iron oxides are inserted. **b** Spectrum of typical chemical composition of crystalline phases in the macrostructure of volcanic ash. The spectrum of calcium alumina silicate was similar to that of pyroxene and the principal differences between the two crystals were their morphologies

plagioclase is adjacent to pyroxene and constitutes an important component of the matrix of fired volcanic ash. The XRD peaks revealed anorthite and anorthoclase (for Z4 and Z6) as well as minor albite (for Z4). It could be possible in some area to identify individual grain of anorthite (Figs. 2b and 3) but generally those grains were embedded in the complex structure, facilitated with the difference in morphology, dimensions and grain sizes, allowing insertion of pyroxene grains in the lattices of skeleton developed by spinel crystals and mass of plagioclase. These spinel crystals seem to grow progressively during sintering and are influenced by the chemical environment as some regions are favorable for the development of large well crystallized grains. All crystals with $(Mg_xFe_{1-x})_2SiO_4$ composition presented ring of Ti-rich micro ferro crystals and oxides which we suggested as nucleating agents. The particularity of these spinel grains is that they are externally formed of a ring of ferro-crystals supported by the matrix [Fig. 3(4)]. Between this ring and the actual $(Mg_xFe_{1-x})_2SiO_4$ structure is another ring completely different from the first with the particularity of having high concentration of Ca^{2+} ions, with decrease in iron content compared to the first ring [Fig. 3(4)]. This structure leads to the hypothesis of a particular mechanism of the synthesis of these crystals. The mechanism by which iron and titanium ions play a special role. Iron play at the same time the role of nucleation and constitutive element as it can be observed from the variation of principal oxides in the spinel crystal of Fig. 3(4). This variation and the pure chemical composition of spinel make us assume the nucleation phenomenon as well as selective diffusion of ions participate in the mechanism of growth of spinel crystals. Its dimension that varies should be ascribed to the chemical

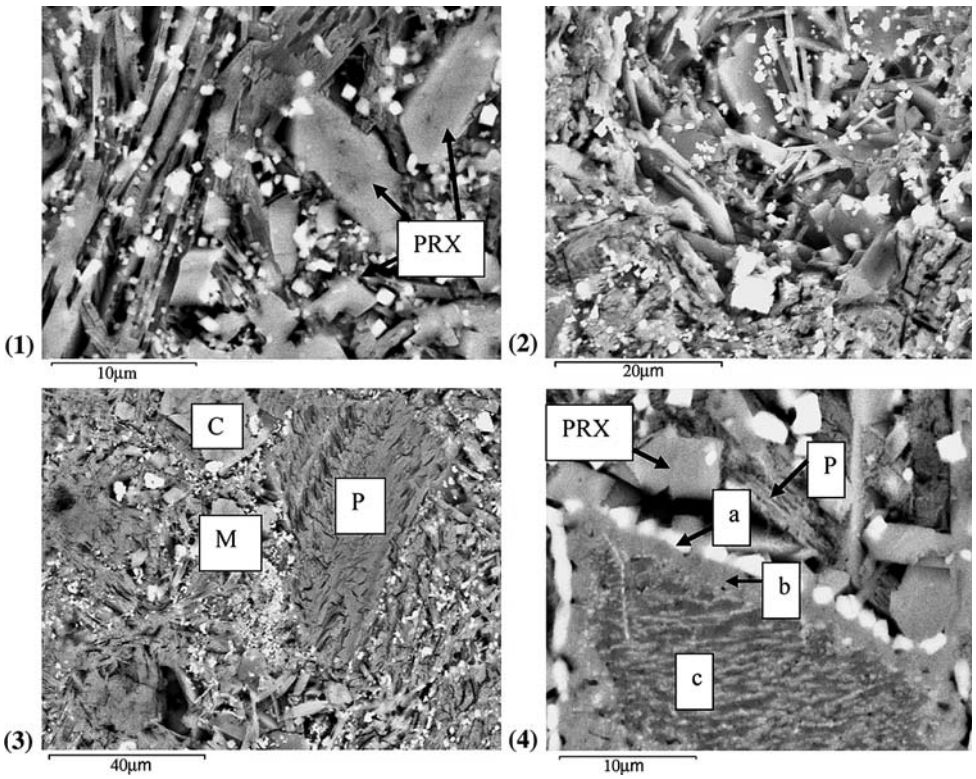

Fig. 3 The interlocking of crystalline phases in the contiguous matrix is more visible at high magnification: pyroxene, Ti-rich ferro crystals (FC) and oxides are dispersed in the matrix (**1**, **2** and **3**) which are collected from P1, P3 and P5, respectively. In **4**, variation in oxides of different regions of spinel from the external (a) to the centre of the crystal (c) via intermediate ring (b), suggesting particular crystallization mechanism with Ti-rich iron particles as nucleating agents

environment of nucleoids formed or already existing in raw materials. In the regions of concentrated glassy phase, Ti-rich iron crystals and oxides were homogeneously dispersed but the chemical composition here slowly differs from that rounding spinel crystals (Fig. 4b). The promotion in these regions of dendrites that continuously grow to pyroxene confirmed well the nucleation role of these groups of crystals (Fig. 4). In the regions of concentration of plagioclase and well crystallized pyroxene, these micro crystals were almost absent. This concludes the role that play the liquid phase on the initiation of dendrites and continuous crystallization. This liquid phase is responsible for the dissolution of the rare grains of quartz present in the structure. But any small inhomogeneity can influence this dissolution as it was observed in a previous work [10] where ferro crystals in the region of closed porosity are responsible for the low viscosity for a liquid phase in a region where quartz grain is partially dissolved. Some authors demonstrated the role of liquid phase as well as that of iron ions ($Fe^{2+/}Fe^{3+}$) in the crystallization behavior of pyroxene [2, 3, 12]. The iron oxides and Ti-rich iron crystals may affect glass stability in at least two manners, by its amount, and by the Fe^{2+}/Fe^{3+} ratio, the oxygen content of the firing atmosphere defines the oxygen potential toward the glass which in turn may affect the crystallization. Burkhard [3] noted the difference in crystallization behavior and resulting textures of Fe^{3+}-rich basalt compared to Fe^{2+}-rich based. The difference comes from the presence of pyroxene, plagioclase and Fe–Ti oxides in the first and only pyroxene and Fe–Ti oxides for the second with grain sizes that grow with temperature.

As reported in the previous work [9], the water absorption of fired volcanic ash is under 1.5% at 1150 °C, which is in agreement with the ISO 13006 for the unglazed tiles class BI. The total porosity was low (<3%) at the same temperature allowing comparison with high quality vitrified conventional ceramic [13]. The lower porosity obtained at 1150 °C was correlated to the maximum shrinkage and densification [9]. The disappearance of pores in the range of temperature 1125–1150 °C enhanced crystallization with possible grain growth and maximum packing. As a consequence, in this range of temperatures, product with good ceramic properties and microstructure is obtained. The microstructural investigation revealed essentially round pores generally <10 μm identified to be mostly intergranular pores that ought to have relation with the high degree of crystallization of fired volcanic ash [9,

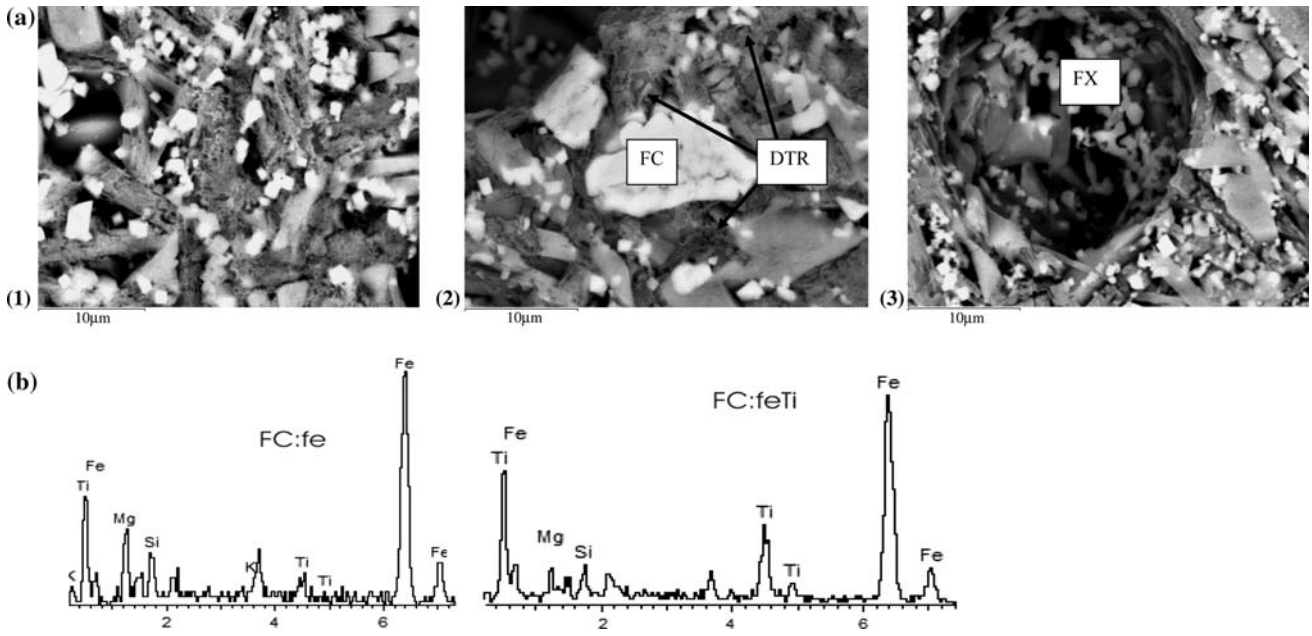

Fig. 4 **a** Precipitation of dendrites (DTR) in the matrix and regions of glass concentration with probable influence of Ti-rich iron crystals and oxides as nucleating agents (**1**, **2**, **3**). Crystallization of spheroidal grains of iron compounds (FX) in the regions of glass concentration (**3**) exposed by etching. These iron compounds are different from those concentrated around spinels (FC). **b** Spectrum of iron compounds: FC:FeTi is that of FC crystals regularly present at the surface of spinel grains and some regions of the matrix as well as in glass concentration regions; FC:fe is that of spheroidal grains of iron compounds present essentially in the glass concentration regions

10]. The absence of volatile compounds in the volcanic ash and their sintering mechanism reduced the possibilities of pores resulting from the gas liberation. Situation that contributes to simplify the thermal cycle of the fired volcanic ash.

Micro hardness and fracture mechanic observations

The variation of the micro hardness behavior of fired volcanic ash was carried out at room temperature and is shown in Table 1 where the various fracture toughness calculated from the values of micro hardness obtained for the specific thermal cycle applied are presented. The hardness decreased with increasing load and is influenced by the difference of $Na_2O + K_2O$ amount in the samples Z4 and Z6 and thermal cycle applied. It has been demonstrated that the difference of the amount of alkali in Z4 and Z6 justifies the early vitrification of Z4 and its poor ceramic properties at 1150 °C when the same thermal cycle is applied [9]. As seem in Table 1, there is correlation between expansion behavior, micro hardness and Young's modulus as well as fracture toughness which is in agreement with the suggestion concerning the influence of thermal cycle on the sintering behavior of volcanic ash. Young's modulus is in the range of those of porcelainized tiles and white ware [13]. Figure 5 shows micrographs of samples after indentations. Generally micro hardness is sensible to regions with high concentration of plagioclase, crystals of spinel, dense matrix or glass concentration or pores. This results in differences and real range of errors between each series of 20 indentations considered during every experimentation.

From the microstructural point of view, the fracture surface of volcanic ash ceramic is comparable to that of polycrystalline phases materials with, as it can be observed in Fig. 6, difficulty to identify the markings fracture as it is the case with brittle materials [13]. The presence of pores, the difference in thermal expansion between the crystalline phases and the glass concentration in some regions are all interpreted as cracks origin even if volcanic ash ceramic is in a suitable range of temperatures described as homogeneous materials at the macroscopic point of view. As can be observed in Fig. 5, the inhomogeneity of the materials at the microstructural level results in the inhomogeneity of mechanical properties (toughness). In brittle polycrystalline materials, the microstructure affects the indentation cracks in a number of ways, such as crack termination at porosity and/or grain boundaries normal to the crack path and crack deflection along grain boundaries.

The effect of the microstructure depends on the size and the density (anorthite: 2.75 g/cm^3 and pyroxene 3.5 g/cm^3) of the dominant microstructural features relative to the indent size. Thus, if the average grain size is very much greater than the indent size, an indent in grain will give a toughness similar to the single crystal toughness. This can

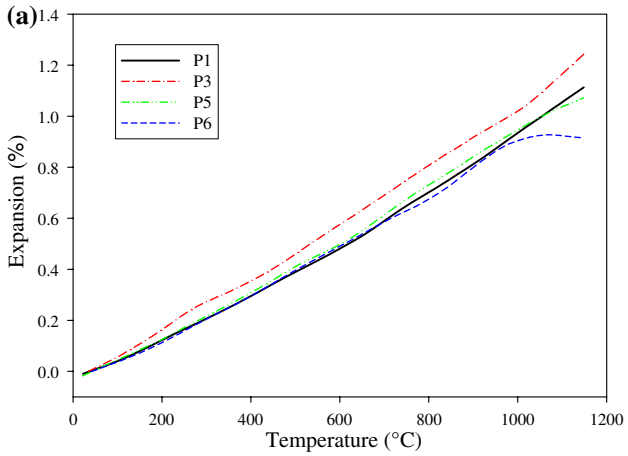

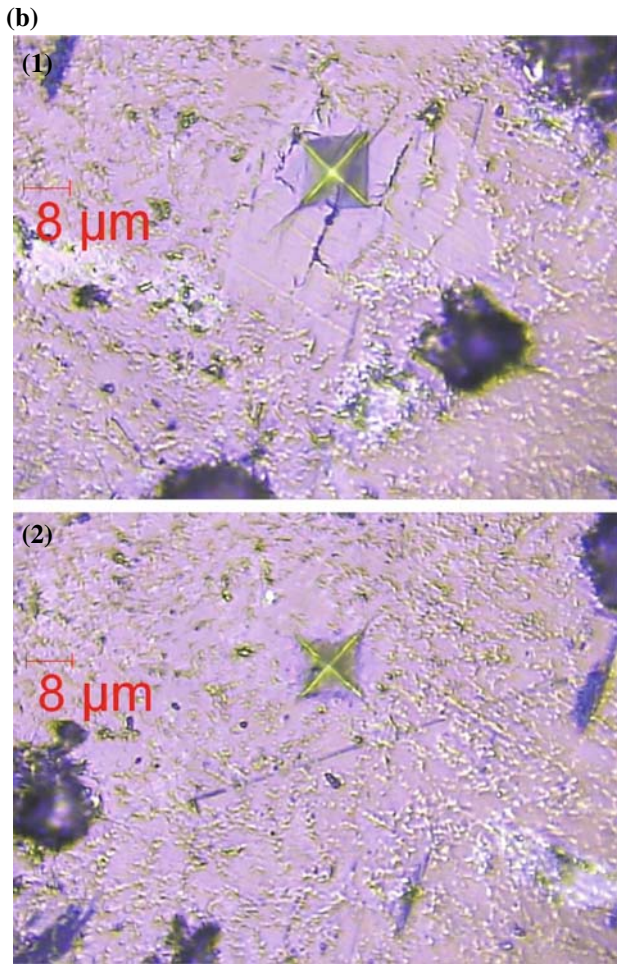

Fig. 5 **a** Thermal expansion behavior of volcanic ash as a function of thermal cycle (P1, P3, P5, P6). **b** Micrographs of the indentation impression performed on the section of fired volcanic ash. **1** 10 N with cracks appearance; **2** 5 N

explain some important variations of the micro hardness and that of the fracture toughness, probably due to some larger (20–50 μm) crystals with chemical composition

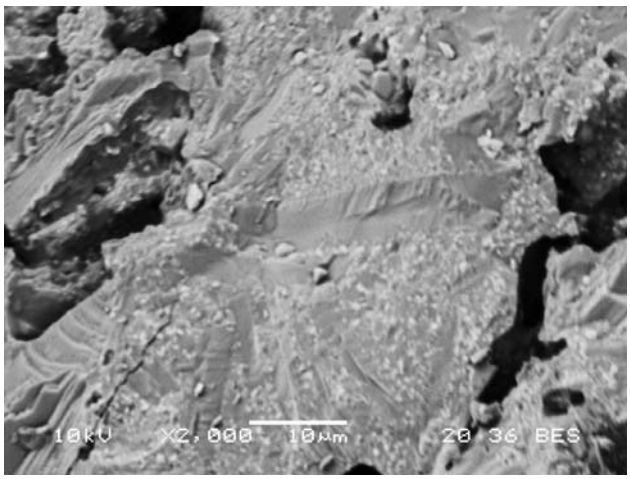

Fig. 6 Fracture surface of volcanic ash ceramics showing mist and twist hackles, inter and transgranular fractures in several places of the micrograph. Regions of cleavage-like steps are observed

$(Mg_xFe_{1-x})SiO_4$ whose values should be greater than those of normal matrix. At the same time the micro heterogeneity described above ought to affect the micro hardness as well as fracture toughness. Indents at the grain boundary intersections or on grain boundaries will give anomalous toughness and crack data. Thus, the homogeneity of the microstructure has an influence on the fracture mechanics of volcanic ash ceramic. Apart from the thermal cycle, the composition influences the critical parameters that are source of cracks and consequently results in the variation of intrinsic properties such as Young's modulus and fracture toughness as function of the thermal expansion (Table 1). Figure 6 shows mist hackle on a fracture surface of volcanic ash ceramic. Twist hackle is present at several places on the large hackle that runs diagonally through the micrographs in addition to inter and transgranular fractures. Mist and velocity hackle and Wallner lines readily seen in these fine grain materials allow comparison with the fracture surface of porcelain and other brittle materials [13–19]. From the examination of fracture surfaces of volcanic ash ceramic and based on the microstructural investigation, it can be pointed that the fracture mechanics of these materials is influenced by the high concentration of crystalline phases and the fracture origin is concentrated on the pores and glass concentration regions which are responsible for micro cracks and cracks.

Discussion and conclusion

From a microstructural point of view, fired volcanic ash is a heterogeneous material with intensive crystalline phases and micro pores dispersed in a dense glassy matrix. The

major phases are minerals of pyroxene group that form with plagioclase a dense network. Crystals of spinel system are regularly dispersed in the matrix and responsible for a homogeneously dispersion of micro Ti-rich iron crystals and oxides. Quartz grains are rarely present in the material making it an outstanding ceramic matrix with respect to the microstructure of conventional vitrified ceramic where quartz plays the important role of a filler. The microstructural study revealed regions with high concentration of glass where micro Ti-rich iron crystals are homogeneously dispersed and probably responsible for the germination, in these regions and in the matrix when the thermal cycle is favorable, of dendrites that continuously grow to pyroxene. The presence of the intensive crystalline phases along with dendrites conferred to the volcanic ash ceramic a dense and contiguous structure where mechanical properties (strength [9, 10], Young's modulus, fracture toughness) contrast with relative low sintering temperature, although at this low temperature the fracture surface confirmed, with fracture analysis, the good densification of the materials during firing. The mechanism of formation of these dendrites and that of crystallization of spinel suggest the possible diffusion phenomenon during the development of the microstructure of fired volcanic ash as identified above (Fig. 4). This mechanism has been described by many authors [2, 4, 5, 20]. The FeO:Fe_2O_3 ratio, the Ti^{4+} and the relative amount of $Na_2O + K_2O$ play important roles on their nucleation and the formation of fine grained microstructures [2, 7]. Because of the chemical environment and the micro inhomogeneity of fired volcanic ash, the size of crystals of spinel (or olivine) varies from small particles of 2 μm to larger grains of 20–50 μm. The formation of well crystallized and pure pyroxene grains in an isolated pores (Fig. 4a) with glass concentration confirmed the influence of liquid phase on the synthesis of pyroxene. The influence of alkali on the formation of dendrites that continuously grow to pyroxene can be compared to the role of the same alkali on the fluidity of glassy phase of porcelain that is known to favor the growth of secondary mullite crystals from clay and feldspar relicts [14, 15]. Eutectic liquid is necessary for the precipitation of secondary mullite in vitrified kaolin [16]. The amount of liquid formed at sintering temperature, and the duration at which the crystallization has taken place, will determine the chemical composition and the aspect and ratio of secondary mullite. Comparatively, Torres and Alarcon [2] demonstrated that in the quaternary system CaO–MgO–Al_2O_3–SiO_2, a small amount of alkaline oxides is required to maximize crystallization and to develop crystals with well-shaped morphologies. Burkhard [17] noted that this crystallization starts, in the case of basalts glasses, with the formation of pyroxene dendrites and Fe–Ti oxides at their apices below 840 °C. Above 920 °C, crystallization of pyroxene occurs with additional plagioclase. Shen et al. [18] showed that dendrites generally developed three branches. These branches with 90° or 110° angles between them grow preferably along with clinopyroxene crystal axis.

Fired volcanic ash contains high viscous glassy matrix. Its properties are directly influenced by the continuous concentration of glass. The thermal cycle applied can increased this glass concentration or enhance crystallization. The glass regions where nucleation will not take place should be necrotic for existing crystalline phases. These regions increase with temperature because of crystals dissolution. The difference on composition and size of crystalline phases in the microstructure of fired volcanic ash results in the difference on the remaining glass and we can conclude on the inhomogeneity of these glassy regions. Glassy regions with high concentration of iron have been identified whereas others presented less iron and calcium ions. This inhomogeneity is caused by the dissolution of crystalline phases in some regions compared to others as a function of the thermal cycle. The most homogeneous glassy phase and matrix is obtained when controlled sintering is developed. The good ceramic properties with relevant microstructure compares well to that of glass-ceramic materials with fracture toughness and fracture surface comparable to that of porcelain [13, 19].

Acknowledgement This work was assisted financially by the University of Modena and Reggio Emilia.

References

1. Leonelli C, Manfredini T, Paganelli M, Pozzi P, Pellicani GC (1991) J Mater Sci 26:5041. doi:10.1007/BF00549889
2. Torres FJ, Alarcon J (2004) J Non-Cryst Solids 347:45
3. Burkhard DJM, Scherer T (2006) J Non-Cryst Solids 352:3961
4. Polettini A, Poni R, Trini L, Muntoni A, Lo Mastro S (2004) Chemosphere 56:901
5. Pisciella P, Pelino M (2005) J Eur Ceram Soc 25:1861
6. Barbieri L, Corradi AB, Lancellotti I (2000) J Eur Ceram Soc 20:1637
7. El-Shennawi AWA, Mandour MA, Morsi MM, Abdel-Hameed SAM (1999) J Am Ceram Soc 82(5):1181
8. Francis AA, Rawlings RD, Sweeney R, Boccaccini AR (2004) J Non-Cryst Solids 333:187
9. Leonelli C, Kamseu E, Boccaccini DN, Melo UC, Rizzuti A, Billong N, Miselli P (2007) Adv Appl Ceram 106:135
10. Kamseu E, Boccaccini D, Sola A, Rizzuti A, Leonelli C, Melo UC, Billong N (2008) Adv Appl Ceram 107:19
11. Marshal DB, Tatsuo N, Evans AG (1982) J Am Ceram Soc 65:C-175
12. Aoki K-I, Shibi I (1973) Lithos 6:41
13. Schneider SJ Jr et al (1987) Glass and ceramics, vol 4. Engineering materials handbook. ASM International
14. Schuller KH (1964) Trans Br Ceram Soc 63(2):103
15. Urbain G, Cambier F, Deletter M, Anseau MR (1981) Trans J Br Ceram Soc 80:139

16. Lu H-y, Wang W-L, Tun W-H, Lin M-H (2004) J Am Ceram Soc 87(10):1843
17. Burkhard DJM (2001) J Petrol 42(3):507
18. Shen S, Zhao S, Zhang S (1998) China University of Geosciences, Wuhan, People's Republic of China, Kuangwu, vol 18(1), p 23
19. Fréchette VD (1990) Failure analysis of brittle materials, vol 28. Advances in ceramics. The American Ceramic Society
20. Karamanov P, Pisciella M, Pelino J (1999) Eur Ceram Soc 19:2641